Theoretical Study of the Reaction of $B_{20}H_{16}$ with MeCN: *Closo/Closo* to *Closo/Nido* Conversion

Oottikkal Shameema, Biswarup Pathak, and Eluvathingal D. Jemmis*

Department of Inorganic and Physical Chemistry, Indian Institute of Science, Bangalore 560-012, India

We propose a mechanism for the cage-opening reaction of a four atoms shared *closo/closo* $B_{20}H_{16}$ (**1**) with MeCN to a face shared *closo/nido* macropolyhedron $B_{20}H_{16}(MeCN)_2$ (**4**) through a diamond-square-diamond rearrangement. Even though only one isomer of the product has been reported experimentally, our computational studies at the B3LYP/6-31G* level predict the possibility of the formation of the other isomers. Depending upon the position of the attack of the MeCN ligand on the polyhedral skeleton, different products are formed. The energetics of the reactions of $B_{20}H_{16}$ with Me_2S and H_2O are comparable.

Introduction

Monopolyhedral boranes are extensively studied both theoretically and experimentally.[1] The structure and electronic structure relationships of monopolyhedral boranes have evolved over the years from the works of Lipscomb,[2a] Hoffmann,[2b] Mingos,[2c] Rudolph,[2d] Williams,[2e] Hawthorne,[2f] Grimes,[2g] and especially Wade.[2h,i] The Wade's rules guided the chemistry of polyhedral boranes, carboranes, and metallaboranes.[2i] Monopolyhedral boranes condense in different ways giving single atom sharing, edge sharing, face sharing, and four atoms sharing macropolyhedral boranes. The first synthesized *closo* macropolyhedron, $B_{20}H_{16}$[3] (**1**, Figure 1), has four atoms shared between two icosahedral units. This is the smallest *closo* macropolyhedron involving two icosahedral units. The lack of charge was thought to be unusual as *closo* boranes are known to have −2 charges. Our attempt to organize and rationalize the structure of the macropolyhedral boranes led to the *mno* rule.[4] Application of the *mno* rule (where m = number of polyhedra, n = number of vertices, and o = number of single atom sharing) indicates that $B_{20}H_{16}$ is neutral.[4b]

The *mno* rule also predicted that the next analogue, a three atoms shared condensed structure, *closo/closo* $B_{21}H_{18}^{1-}$ (**2**, Figure 1) is negatively charged. Despite the initial success in the synthesis of $B_{20}H_{16}$ 40 years ago, the developments of the chemistry of macropolyhedral boranes were very slow during the next 20 years. However, during the last 25 years, there have been dramatic developments in the chemistry of macropolyhedral boranes. There are several reasons for this. First of these is the realization that macropolyhedral boranes are the ideal candidates in the boron neutron capture therapy (BNCT) of cancer.[5] The larger the number of boron atoms in the molecule, the better is the efficiency of the treatment. A second impetus came from the development in metall-

* To whom correspondence should be addressed. E-mail: jemmis@ipc.iisc.ernet.in. Fax: 91-80-2360-1552.

(1) (a) Williams, R. E. *Chem. Rev.* **1992**, *92*, 177. (b) King, R. B. *Chem. Rev.* **2001**, *101*, 1119.

(2) (a) Eberhardt, W. H.; Crawford, B.; Lipscomb, W. N. *J. Chem. Phys.* **1954**, *22*, 989. (b) Stohrer, W. D.; Hoffmann, R. *J. Am. Chem. Soc.* **1972**, *94*, 1661. (c) Mingos, D. M. P.; Wales, D. J. *Introduction to Cluster Chemistry*; Prentice Hall: Englewood Cliffs, NJ, 1990. (d) Rudolph, R. W. *Acc. Chem. Res.* **1976**, *9*, 446. (e) Williams, R. E. In *Progress in Boron Chemistry*; Brothertonand, R. J., Steinberg, H., Eds.; Pergamon: Oxford, U.K., 1970; Vol. *II*, p 37. (f) Evans, J. W.; Hawthorne, M. F. *Inorg. Chem.* **1973**, *13*, 870. (g) Grimes, R. N. *Carboranes*; Academic Press: New York, 1970. (h) Wade, K. *Electron Deficient Compounds*; Nelson: London, 1971. (i) Olah, G. A.; Wade, K.; Williams, R. E. *Electron-Deficient Boron and Carbon Clusters*; Wiley: New York, 1991.

(3) (a) Miller, N. E.; Muetterties, E. L. *J. Am. Chem. Soc.* **1963**, *85*, 3506. (b) Friedman, L. B.; Dobrott, R. D.; Lipscomb, W. N. *J. Am. Chem. Soc.* **1963**, *85*, 3505. (c) Miller, N. E.; Miller, C. H.; Muetterties, E. L. *Inorg. Chem.* **1964**, *3*, 1690. (d) Dobrott, R. D.; Friedman, L. B.; Lipscomb, W. N. *J. Chem. Phys.* **1964**, *40*, 866.

(4) (a) Jemmis, E. D.; Balakrisnaranjan, M. M.; Pancharatna, P. D. *J. Am. Chem. Soc.* **2001**, *123*, 4313. (b) Jemmis, E. D.; Balakrisnaranjan, M. M.; Pancharatna, P. D. *Chem. Rev.* **2002**, *102*, 93. (c) Jemmis, E. D.; Jayasree, E. G. *Acc. Chem. Res.* **2003**, *36*, 816. (d) Balakrishnarajan, M. M.; Jemmis, E. D. *J. Am. Chem. Soc.* **2000**, *122*, 4516.

(5) (a) Feakes, D. A.; Shelly, K.; Knobler, C. B.; Hawthorne, M. F. *Proc. Natl. Acad. Sci. U.S.A.* **1994**, *91*, 3029. (b) Hosmane, N. S.; Franken, A.; Zhang, G.; Srivastava, R. R.; Smith, R. Y.; Spielvogel, B. F. *Main Group Met. Chem.* **1998**, *21*, 319. (c) Shelly, K. J.; Hawthorne, M. F.; Schmidt, P. G. In *Progress in Neutron Capture Therapy*; Allen, B. J., Moore, D. E., Harrington, B. V., Eds.; Plenum: New York, 1992; p 259. (d) Luqman, A.; Sumathy, N. H.; Eklund, J. E.; Wang, J.; Hosmane, N. S. *J. Am. Chem. Soc.* **2002**, *124*, 7292.
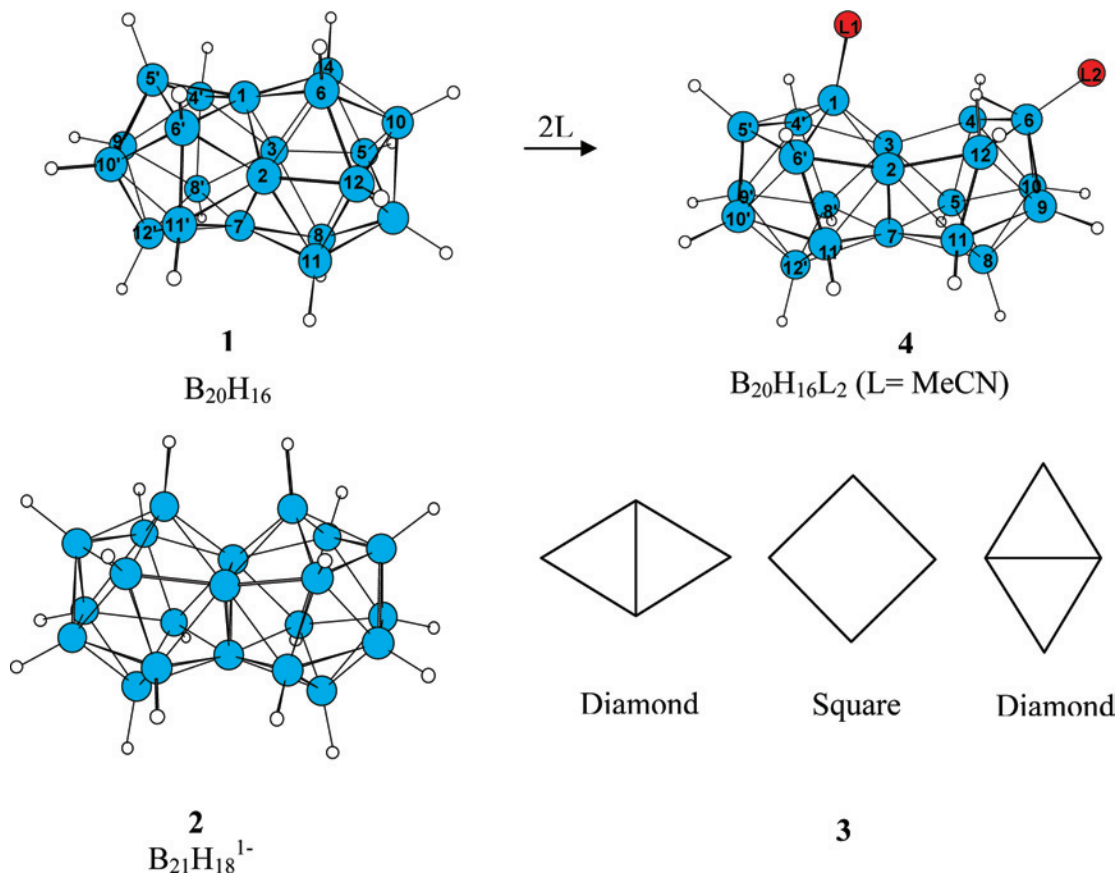
Figure 1. Conversion of *closo/closo* $B_{20}H_{16}$ (**1**) to *closo/nido* $B_{20}H_{16}L_2$ (**4**), structure of $B_{21}H_{18}^{1-}$ (**2**), and the scheme showing the diamond-square-diamond (DSD) rearrangement (**3**).

aboranes. The painstaking experimental works of Fehlner for the synthesis of metallaboranes,[6] the methodologies introduced by Kennedy for condensation of metallaboranes into macropolyhedral structures,[7] and the strategies evolved by Welch in synthesizing supra-icosahedral metallaboranes[8] are the landmarks in this development. The *closo/closo* macropolyhedral structure, with a shared triangular face between two icosahedra, $B_{21}H_{18}^{1-}$ (**2**, Figure 1) was synthesized very recently.[9] Clearly, the synthetic chemistry in this area has a vast horizon to conquer.

Mechanistic studies of the reaction of polyhedral boranes are even more scarce. There is a fascinating account of polyhedral skeleton rearrangement reactions in carboranes. For example $1,2$-$C_2B_{10}H_{12}$ rearranges to $1,7$-$C_2B_{10}H_{12}$ at 470 °C and to $1,12$-$C_2B_{10}H_{12}$ at 700 °C.[10a] The activation energy

barrier for the rearrangement of $1,2$-$C_2B_{10}H_{12}$ to $1,7$-$C_2B_{10}H_{12}$ is calculated to be 62.0 kcal/mol.[10b] Out of the many proposed mechanisms, the diamond-square-diamond (DSD)[11] (**3**, Figure 1), the local bond rotation,[12] and the *closo-nido-closo* rearrangements[13] are the generally accepted reaction pathways for polyhedral rearrangements. The DSD rearrangements have been used in rationalizing a number of isomerizations found in borane, carboranes, metallaboranes, and metallacarboranes.[14]

The rearrangement reactions of macropolyhedral boranes are found to be much more intriguing. The $B_{20}H_{16}$ (**1**) is known to react[15] with MeCN and Me$_2$S without the loss of hydrogen, giving three atom shared *closo/nido* $B_{20}H_{16}L_2$ (**4**, Figure 1). The reaction has been known for more than 40 years, and one of the products has been characterized. More recently, the chem-

(6) Fehlner, T. P. In *Group 13 Chemistry: From Fundamentals to Applications*; Shapiro, P. J., Atwood, D. A., Eds.; American Chemical Society: Washington, DC, 2002; p 49.

(7) (a) Bould, J.; Kennedy, J. D.; Thornton-Pett, M. *J. Chem. Soc., Dalton Trans.* **1992**, 563. (b) Kennedy, J. D.; Sÿtibr, B. In *Current Topics in the Chemistry of Boron*; Kabalka, G. W., Ed.; Royal Society of Chemistry: Cambridge, U.K., 1994; pp 285−292. (c) Kennedy, J. D. In *The Borane-Carborane-Carbocation Continuum*; Casanova, J., Ed.; Wiley: New York, 1998; Chapter 3, pp 85−116. (d) Sÿtibr, B.; Kennedy, J. D.; Drda′kova′, E.; Thornton-Pett, M. *J. Chem. Soc., Dalton Trans.* **1994**, 229.

(8) (a) McIntosh, R. D.; Ellis, D.; Rosair, G. M.; Welch, A. J. *Angew. Chem., Int. Ed.* **2006**, *45*, 4313. (b) McIntosh, R. D.; Ellis, D.; Rosair, G. M.; Welch, A. J. *Angew. Chem., Int. Ed.* **2003**, *42*, 225. (c) Wilson, N. M. M.; Ellis, D.; Boyd, A. S. F.; Giles, B. T.; Macgregor, S. A.; Rosair, G. M.; Welch, Al. J. *Chem. Commun.* **2002**, 464.

(9) Bernhardt, E.; Brauer, D. J.; Finze, M.; Willner, H. *Angew. Chem., Int. Ed.* **2007**, *46*, 2927.

(10) (a) Papetti, S.; Heyling, T. L. *J. Am. Chem. Soc.* **1964**, *86*, 2295. (b) Salinger, R. M.; Frye, C. L. *Inorg. Chem.* **1965**, *4*, 1815.

(11) Lipscomb, W. N. *Science* **1966**, *153*, 3734.

(12) (a) McKee, M. L. *J. Am. Chem. Soc.* **1988**, *110*, 5317. (b) McKee, M. L. *J. Am. Chem. Soc.* **1992**, *114*, 879.

(13) (a) Graham, G. D.; Marynick, D. S.; Lipscomb, W. N. *J. Am. Chem. Soc.* **1980**, *102*, 2939. (b) Wong, H. S.; Lipscomb, W. N. *Inorg. Chem.* **1975**, *14*, 1350.

(14) (a) Wade, K. In *Electron Deficient Compounds*; Nelson: London, 1971. (b) Kennedy, J. D. In *Progress in Inorganic chemistry*; Wiley: New York, 1986; Vol. *34*. (c) Gimarc, B. M.; Warren, D. S.; Ott, J. J.; Brown, C. *Inorg. Chem.* **1991**, *30*, 1598. (d) McKee, M. L. *J. Am. Chem. Soc.* **1995**, *117*, 8001. (e) Wales, D. J.; Bone, R. G. A. *J. Am. Chem. Soc.* **1992**, *114*, 5399. (f) Zhao, M.; Gimarc, B. M. *Polyhedron* **1995**, *14*, 1315. (g) McKee, M. L. *J. Am. Chem. Soc.* **1992**, *114*, 879.

(15) (a) Friedman, L. B.; Enemark, J. H.; Lipscomb, W. N. *Inorg. Chem.* **1966**, *5*, 2165. (b) Enemark, J. H.; Friedman, L. B.; Hartsuck, J. A.; Lipscomb, W. N. *J. Am. Chem. Soc.* **1966**, *88*, 3659.

istry of B$_{20}$H$_{16}$ is further explored[16] by the reaction with [ReH$_5$(PMe$_2$Ph)$_3$], leading to a 21 vertex, three atom shared, *closo/nido* metallaborane. A rich macropolyhedral chemistry involving rearrangements in thiaborane and metallaboranes has been developed by Kennedy and co-workers.[17] Conversion of the nineteen vertex metallaboranes, [(η^5-C$_5$Me$_5$)IrB$_{18}$H$_{20}$], with a triangular face sharing to a 20 vertex edge sharing [(η^5-C$_5$Me$_5$)IrB$_{18}$H$_{19}$S]$^-$ anion has been reported.[18a] It is pointed out that the reductive addition of electron rich sulfur reduces the number of shared atoms in the cluster bonding. The reaction of PMe$_2$Ph with the three atoms shared metallaborane, [(η^5-C$_5$Me$_5$)IrB$_{18}$H$_{20}$], also results in the two atoms shared macropoly-hedron, [(η^5-C$_5$Me$_5$)IrB$_{18}$H$_{19}$(PHPh$_2$)].[18b] In these reactions, the addition of ligands to the condensed cluster leads to a decrease in the number of shared atoms. Rearrangement reactions of macropolyhedral metallaboranes show that the presence of transition metal centers in the macropolyhedral boranes can induce considerable additional flexibility for the generation of novel clusters. The recently reported[9] weakly coordinating *closo* anion [B$_{21}$H$_{18}$]$^{1-}$ is synthesized from the three atoms shared *closo/nido* [B$_{20}$H$_{18}$]$^{2-}$ dianion, which is structurally and elec-tronically equivalent to B$_{20}$H$_{16}$L$_2$. In view of the reaction of B$_{20}$H$_{16}$ with Lewis bases giving B$_{20}$H$_{16}$L$_2$, it is pointed out that the B$_{20}$H$_{16}$ can be used as a starting point. Hillebrecht et al.[19] reported the synthesis and crystal structure of MgB$_{12}$, which consists of a three-dimensional net of B$_{12}$ icosahedra and B$_{21}$ units in the ratio 2:1. Here, the B$_{21}$ units consist of *closo/nido* B$_{20}$ units, which are structurally similar to the B$_{20}$H$_{16}$L$_2$ skeleton. Functionalization of the macropolyhedral borate anion cluster [B$_{22}$B$_{22}$]$^{2-}$ as OH and OEt derivatives has been reported by Barton et al.[20] The two-electron reductive cage-opening and metalation of *closo* carboranes have been well documented in the literature.[21] Thus, the era of macropolyhedral borane chemistry has begun.

The detailed mechanisms of the individual reactions in the macropolyhedral boranes are only beginning to be explored. The multiple possibilities for the reaction pathways have made mechanistic studies very difficult. As a prelude, to understand the complex mechanistic details of the reactions of macropolyhedral boranes, we have undertaken a study of the reaction of B$_{20}$H$_{16}$ (**1**) with MeCN. Even for this substrate,
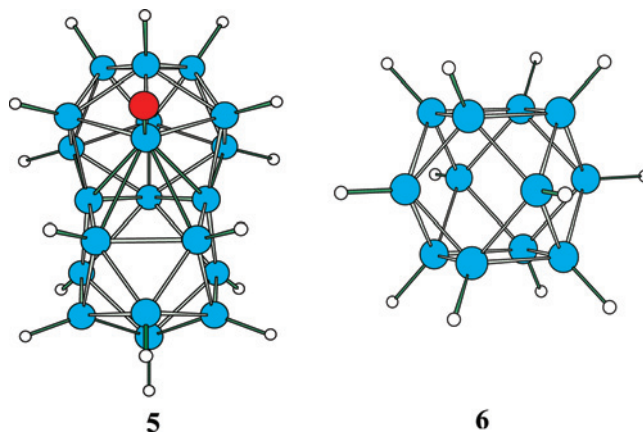
Figure 2. Cuboctahedron structures for B$_{20}$H$_{16}$L (**5**) and B$_{12}$H$_{12}$$^{2-}$ (**6**).

the number of possible reaction pathways is very large, and we have tried to be as exhaustive as possible in the theoretical analysis of the reaction. An increasing knowledge of the mechanistic details of the reactions of polyhedral boranes is sure to encourage further exploration in this developing area.

Lipscomb has proposed[11,15] a mechanism for the ring opening of B$_{20}$H$_{16}$ (**1**) in the presence of MeCN, which involves four diamond-square-diamond (DSD) rearrange-ments. The mechanism involves the nucleophilic attack of MeCN at one of the shared boron atoms of B$_{20}$H$_{16}$ (**1**) followed by DSD rearrangements leading to an intermediate where one of the icosahedra has cuboctahedral geometry (**5**, Figure 2). The breaking of three B–B bonds of the cuboctahedron intermediate leads to the *closo/nido* structure (**4**), but a detailed quantitative study of this structural rearrangement is not available. We present a detailed theoretical study of the mechanism for the rearrangement of *closo/closo* B$_{20}$H$_{16}$ (**1**) to *closo/nido* B$_{20}$H$_{16}$L$_2$ (**4**) in the presence of L = MeCN. This involves a DSD rearrangement but not the one suggested earlier. A detailed understanding of this reaction would help in the study of more complex rearrangements of metallaboranes and macropolyhedral boranes especially in studying the reactivities of B$_{21}$H$_{18}$$^{1-}$ (**2**), synthesized recently.

Computational Methods. The geometries of all the structures involved in the addition of MeCN, Me$_2$S, and H$_2$O to B$_{20}$H$_{16}$ are optimized using the hybrid HF-DFT method, B3LYP/6-31G*. This is based on Becke's three parameter functional including the Hartree–Fock exchange contribution

(16) Kaur, P.; Perera, S. D.; Jehnek, T.; Stibr, B.; Kennedy, J. D.; Clegg, W.; Thornton-Pett, M. *J. Chem. Soc., Chem. Commun.* **1997**, 217.

(17) (a) Kaur, P.; Thornton-Pett, M.; Clegg, W.; Kennedy, J. D. *J. Chem. Soc., Dalton Trans.* **1996**, 4155. (b) Kaur, P.; Kennedy, J. D.; Thornton-Pett, M.; Jelinek, T.; Stíbr, B. *J. Chem. Soc., Dalton Trans.* **1996**, 1765. (c) Jelinek, T.; Kilner, C. A.; Barrett, S. A.; Thornton-Pett, M.; Kennedy, J. D. *Chem. Commun.* **1999**, 1905. (d) Shea, S. L.; MacKinnon, P.; Thornton-Pett, M.; Kennedy, J. D. *Inorg. Chim. Acta* **2005**, *358*, 1709. (e) Carr, M. J.; Londesborough, M. G. S.; Mcleod, A. R. H.; Kennedy, J. D. *Dalton Trans.* **2006**, 3624.

(18) (a) Shea, S. L.; McGrath, T. D.; Jelinek, T.; Stíbr, B.; Thornton-Pett, M.; Kennedy, J. D. *Inorg. Chem. Commun.* **1998**, *1*, 97. (b) Shea, S. L.; Jehnek, T.; Perera, S. D.; Stíbr, B.; Thornton-Pett, M.; Kennedy, J. D. *Dalton Trans.* **2004**, 1521.

(19) Adasch, V.; Hess, K. U.; Ludwig, T.; Vojteer, N.; Hillebrecht, H. *J. Solid State Chem.* **2006**, *179*, 2916.

(20) Volkov, O.; Rath, N. P.; Barton, L. *J. Organomet. Chem.* **2003**, *680*, 212.

(21) Hosmane, N. S.; Maguire, J. A. *Eur. J. Inorg. Chem.* **2003**, *22*, 3989.

(22) (a) Becke, A. D. *Phys. Rev. A: At., Mol., Opt. Phys.* **1988**, *38*, 2398. (b) Lee, C.; Yang, W.; Parr, R. G. *Phys. Rev. B: Condens. Matter Mater. Phys.* **1988**, *37*, 785.

(23) Frisch, M. J.; Trucks, G. W.; Schlegel, H. B.; Scuseria, G. E.; Robb, M. A.; Cheeseman, J. R.; Montgomery, J. A., Jr.; Vreven, T.; Kudin, K. N.; Burant, J. C.; Millam, J. M.; Iyengar, S. S.; Tomasi, J.; Barone, V.; Mennucci, B.; Cossi, M.; Scalmani, G.; Rega, N.; Petersson, G. A.; Nakatsuji, H.; Hada, M.; Ehara, M.; Toyota, K.; Fukuda, R.; Hasegawa, J.; Ishida, M.; Nakajima, T.; Honda, Y.; Kitao, O.; Nakai, H.; Klene, M.; Li, X.; Knox, J. E.; Hratchian, H. P.; Cross, J. B.; Bakken, V.; Adamo, C.; Jaramillo, J.; Gomperts, R.; Stratmann, R. E.; Yazyev, O.; Austin, A. J.; Cammi, R.; Pomelli, C.; Ochterski, J. W.; Ayala, P. Y.; Morokuma, K.; Voth, G. A.; Salvador, P.; Dannenberg, J. J.; Zakrzewski, V. G.; Dapprich, S.; Daniels, A. D.; Strain, M. C.; Farkas, O.; Malick, D. K.; Rabuck, A. D.; Raghavachari, K.; Foresman, J. B.; Ortiz, J. V.; Cui, Q.; Baboul, A. G.; Clifford, S.; Cioslowski, J.; Stefanov, B. B.; Liu, G.; Liashenko, A.; Piskorz, P.; Komaromi, I.; Martin, R. L.; Fox, D. J.; Keith, T.; Al-Laham, M. A.; Peng, C. Y.; Nanayakkara, A.; Challacombe, M.; Gill, P. M. W.; Johnson, B.; Chen, W.; Wong, M. W.; Gonzalez, C.; Pople, J. A. *Gaussian 03*, revision B.03; Gaussian, Inc.: Pittsburgh, PA, 2003.
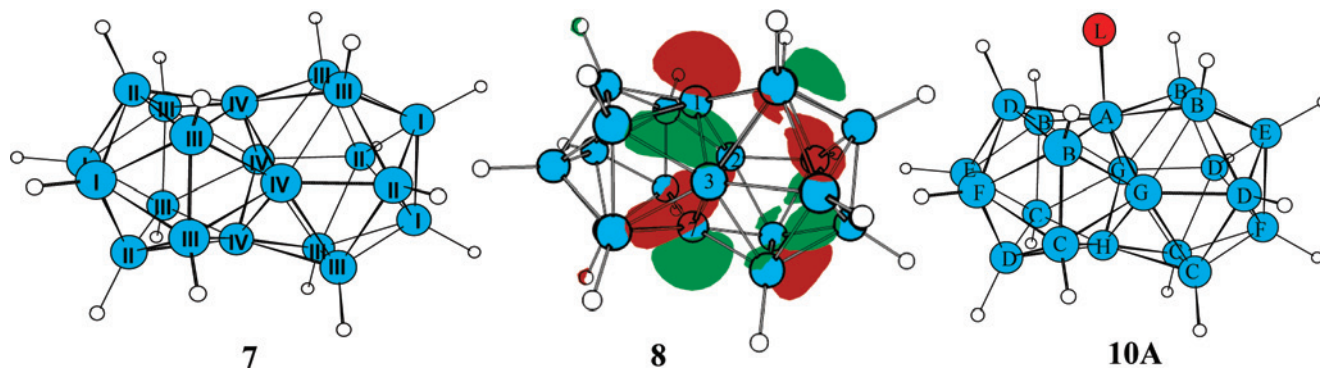
Figure 3. Nonequivalent four types of boron atoms in $B_{20}H_{16}$ (**7**), the lowest unoccupied molecular orbital (LUMO) of $B_{20}H_{16}$ (**8**), and the optimized structure of **10A** showing different possible positions of attack for the second ligand in $B_{20}H_{16}L$.

with a nonlocal correction for the exchange potential proposed by Becke, together with the nonlocal correction for the correlation energy suggested by Lee et al.[22a,b] The nature of the stationary points is characterized by vibrational frequency calculations. All calculations are carried out using the Gaussian 03 suite program.[23]

Results and Discussion

A qualitative analysis of the consequence of the sequential addition of the electron-donating (nucleophilic) reagents on the $B_{20}H_{16}$ (**1**) skeleton is given first. This is followed by the quantitative results of the calculations on the addition of MeCN. There are several symmetrically inequivalent positions in each step of the addition. The four nonequivalent positions in $B_{20}H_{16}$ (**1**) are given in **7** (Figure 3). Out of these, the attack at the position BIV gives the lower energy product (**10A**, Figure 3). The letters **A**, **B**, **C**, and so forth after the numerals indicate the nonequivalent boron atoms in $B_{20}H_{16}L$ (Figure 3). The transition state for the formation of **10A** is labeled as **9A** (**TS**) (Scheme 1). The second attack can take place at any of the seven positions marked as **B- H** (Figure 3). If the second attack takes place at **B**, the product is labeled as **4AB**. After the first step, only the lower energy structures are considered for the next addition. The reaction profile for the addition of three different nucleophiles is compared at the end.

The structural changes due to the addition and removal of electrons in polyhedral boranes can be predicted by electron counting rules. The addition of electrons opens up clusters. For example, the octahedral $B_6H_6^{2-}$ opens up to a *nido* pentagonal pyramid and hexagon (isoelectronic $C_4B_2H_6$ and benzene) by increasing the number of cluster electrons.[2h,4c] The reaction of $B_{20}H_{16}$ with ligand MeCN is equivalent to increasing the number of electrons. The *mno* rule predicts[4b] that the addition of two molecules of MeCN ligand (alternative to adding electrons) to $B_{20}H_{16}$ (**1**) can lead to a structural rearrangement resulting in the three atoms shared *closo/nido* structure (**4**). The *mno* rule demands 23 skeleton electron pairs ($m = 2$, $n = 20$, $o = 0$, $p = 1$, $m + n + p = 23$) for *closo/nido* $B_{20}H_{16}(MeCN)_2$ (**4**). The 15 B−H groups provide 15 electron pairs, and three shared borons provide 4.5 electron pairs. Since the lone pair on the nitrogen is involved in the N^+B^- dative bond, these two boron atoms have an extra electron for skeletal bonding. This adds up to 22.5 electron pairs. The remaining one electron is obtained

from the bridging hydrogen. $B_{20}H_{16}$ (**1**) reacts with water[3c] to form a product of unknown structure with the composition $[B_{20}H_{16}(OH)_2]^{2-}2[H_3O]^+$. Other adducts[3c] such as $[B_{20}H_{16}(OH)_2]^{2-}[N(CH_3)_4]^{2+}$ and $[Cs^+]_2[B_{20}H_{16}(OC_2H_5)_2]^{2-}$, though not characterized experimentally, are also anticipated[4b] to have *closo/nido* structures.

We have studied the energetics of the reaction of $B_{20}H_{16}$ (**1**) with ligand L = MeCN in detail. Obviously, large numbers of individual steps are involved in the conversion of **1** to **4** (Figure 1). The stepwise mechanism suggested by Lipscomb involving cuboctahedron intermediate (**5**, Figure 2) is analyzed first. The cuboctahedron that is located is not an intermediate but a saddle point with three imaginary vibrational frequencies and is 110.0 kcal/mol higher in energy with respect to the reactants. Since the reaction reported by Lipscomb et al. was carried out only at room temperature, the reaction is unlikely to have followed the cuboctahedron path. There is no general agreement on the mechanism involving cuboctahedron intermediates even for the isomerization of $C_2B_{10}H_{12}$.[14c,24] The cuboctahedron structure calculated for $B_{12}H_{12}^{2-}$ (**6**, Figure 2) is a saddle point with four imaginary frequencies and is 121.4 kcal/mol (163.0 kcal/mol, calculated[14c] at HF/4-31G*) higher in energy with respect to icosahedral $B_{12}H_{12}^{2-}$. Hosmane et al.[25] synthesized a novel tetracarborane isomer, $2,4,7,9$-$(SiMe_3)_4C_4B_8H_8$, whose structure is based on the cuboctahedron but contains two additional skeleton electrons than $C_2B_{10}H_{12}$. Therefore, we did not explore the reaction path involving the cuboctahedron intermediate further.

We propose a new mechanism for the conversion of *closo/closo* $B_{20}H_{16}$ (**1**) to *closo/nido* $B_{20}H_{16}L_2$ (**4**), which involves a DSD rearrangement (**3**, Figure 1). The reaction is initiated by nucleophilic attack through the N atom of the ligand MeCN (Scheme 1). There are four nonequivalent boron atoms in $B_{20}H_{16}$ (**7**, Figure 3). Out of these, the shared boron atoms (BIV) have higher positive charge.[15a] The doubly degenerate LUMO of the $B_{20}H_{16}$ (**8**, Figure 3) is mainly concentrated on the four shared boron atoms. So, these boron atoms without hydrogen substituents are more susceptible to nucleophilic attack. However, we have studied the reaction paths that are initiated by the attack

(24) Edvenson, G. M.; Gaines, D. F. *Inorg. Chem.* **1990**, *29*, 1210.
(25) Hosmane, N. S.; Zhang, H.; Maguire, J. A.; Wang, Y.; Thomas, C. J.; Gray, T. G. *Angew. Chem., Int. Ed. Engl.* **1996**, *35*, 1000.

Scheme 1. Proposed Mechanism for the Cage Opening of $B_{20}H_{16}$ (**1**) in the Presence of Ligand, L = MeCN[a]

[a] Ligand L = red, B = blue, and H = white.
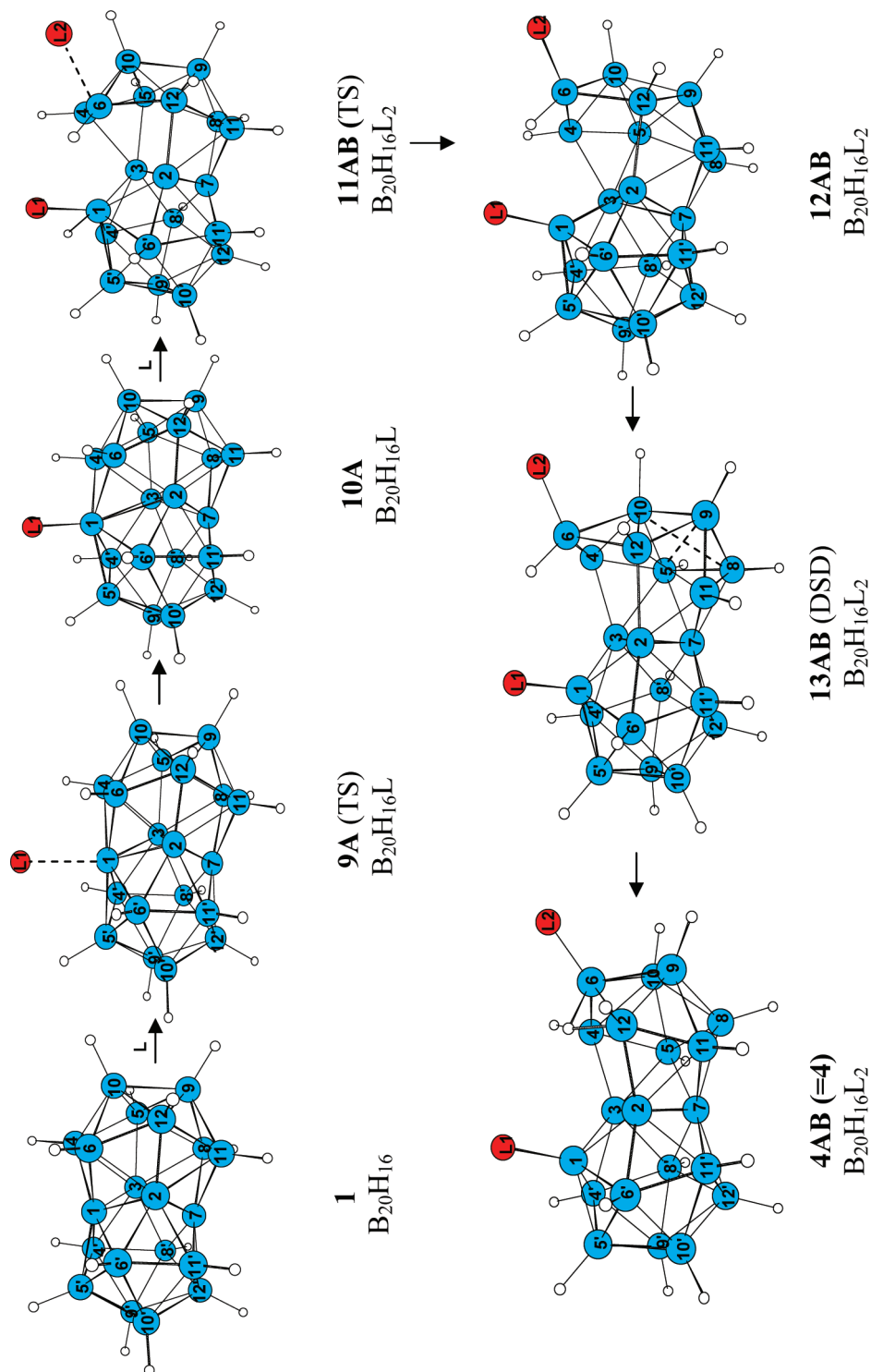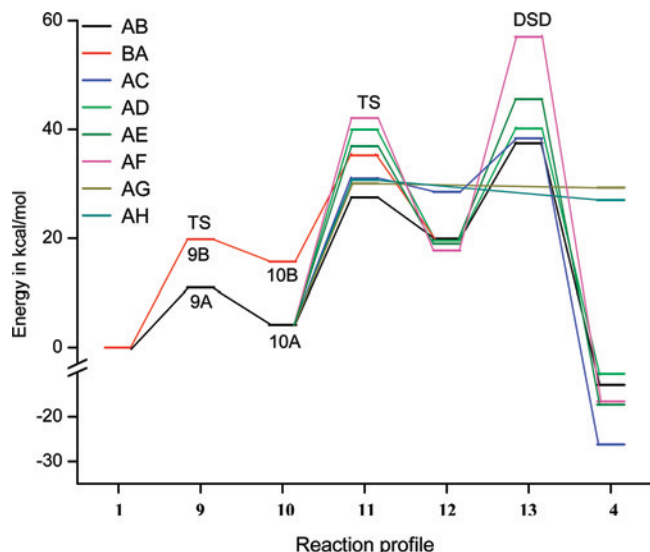
Figure 4. Reaction profile showing energetics of different reaction paths for the attack of MeCN at different types of boron atoms of $B_{20}H_{16}$ giving $B_{20}H_{16}$ (MeCN)$_2$.

Table 1. Relative Energies (kcal/mol) Calculated at the B3LYP/6-31G* Level for Various Structures

structure	AB	AC	AD	AE	AF	AG	AH
1	0.0	0.0	0.0	0.0	0.0	0.0	0.0
9A (TS)	10.9	10.9	10.9	10.9	10.9	10.9	10.9
10A	4.2	4.2	4.2	4.2	4.2	4.2	4.2
11 (TS)	27.1	30.2	40.0	36.2	42.1	30.1	30.7
12	19.9	28.5	19.6	19.7	17.7		
13 (DSD)	37.4	38.4	40.1	45.5	52.0		
4	−12.9	−26.3	−10.4	−17.3	−16.8	29.3	34.8

of the ligand at all the four nonequivalent boron atoms, BI, BII, BIII, and BIV of $B_{20}H_{16}$.

The barriers for the attack of MeCN at BI, BII, BIII, and BIV of $B_{20}H_{16}$ are calculated to be 39.0, 44.6, 19.8, and 10.9 kcal/mol, respectively. Since the barriers of attack at B1 and BII are very high, we did not explore those reaction paths further. The intermediates formed from the attack at BIV and BIII (**10A** and **10B**) are 4.2 and 15.2 kcal/mol higher in energy, with respect to the reactants (Figure 4), clearly indicating that the intermediate **10A** is both thermodynamically and kinetically preferred.

Though the intermediate **10A** appeared to be close to the $B_{20}H_{16}$ (**1**) structure, there are some geometrical changes. The B1−B7 bond length increases by 0.49−0.61 Å, but the B2−B3 bond shortens by 0.29−0.30Å in comparison to the B1−B7 (=B2−B3) bond length of 2.38Å in $B_{20}H_{16}$ (Scheme 1). The molecular orbitals of $B_{20}H_{16}$ show that the LUMO (**8**, Figure 3) is bonding between B2 and B3 and antibonding between B1 and B7, which is responsible for such geometrical changes. However, the intermediate, **10A**, is not isolated in the reaction.

The second ligand, L, adds at another boron atom of **10A** (Figure 3). We have located the transition states for the attack of **10A** (Figure 4) by the second ligand at different positions, and the barriers for these attacks are calculated to be 22.8 (**11AB**), 26.0 (**11AC**), 35.8 (**11AD**), 32.7 (**11AE**), 42.1 (**11AF**), 25.9 (**11AG**), and 26.5 kcal/mol (**11AH**) , respectively (Table 1). The attack of the ligand at **B**, which has the least barrier, leads to the intermediate **12AB**. The attack close to **A**, which has higher coordination number and strain, leads to the easier cluster rearrangement. The structure **12AB** has a *closo* icosahedral {B$_{12}$} unit and a partially opened {B$_{11}$} unit condensed through triangular face sharing. The intermediate **12AB**, which is 19.9 kcal/mol higher in energy than the reactants, undergoes a DSD rearrangement. We have located the transition state for the process, which is higher in energy by 17.5 kcal/mol (**13AB**, Scheme 1). The DSD rearrangement

leads to **4AB** (=**4**), which is a *closo/nido* macropolyhedron and is 12.0 kcal/mol more stable than the reactants. In fact, **4** is the only isomer that is isolated in the experimental study. The transition state corresponds to the DSD rearrangement in the tetragonal face of **13AB** (B5, B8, B9, and B10), shown as a dotted line in the Scheme 1. The DSD rearrangement in **12AB** shortens the B8−B10 distance from 3.01Å to 1.81Å and elongates the B5−B9 distance from 1.83Å to 2.88Å. The DSD rearrangement brings the B10 atom to the plane of B5, B7, B11, and B9 and forms the lower five-membered ring of the {B11} unit to form the *closo/nido* structure. *Closo/nido* structure **4**, has a *closo* {B$_{12}$} icosahedral unit and a *nido* {B$_{11}$} unit fused with a common triangular face. The open face is adjacent to the shared triangle.

The attack of the second ligand at the other possible nonshared boron atoms (**C**, **D**, **E**, and **F**) also proceeds through similar mechanisms. The intermediates formed, **12AC** (28.5), **12AD** (19.6), **12AE** (19.7), and **12AF** (17.7 kcal/mol), are close in energy but have relatively higher transition states of formation than **11AB** (22.9), **11AC** (26.0), **11AD** (35.8), **11AE** (32.0), and **11AF** (26.0 kcal/mol), respectively (Table 1). The intermediates undergo DSD rearrangements with barriers of 9.8 (**13AC**), 20.5 (**13AD**), 25.8 (**13AE**), and 39.3 kcal/mol (**13AF**) leading to different products (Figure 4). All the products formed have *closo/nido* structural patterns (Figure 5) with energies of −26.3 (**4AC**), −10.4 (**4AD**), −17.3 (**4AE**), and −16.8 kcal/mol (**4AF**), respectively, with respect to reactants. In order to justify the relative energies of these different isomers, a detailed analysis on the effect of substitution on the macropolyhedral skeleton is needed. Even though the products **4AC** and **4AE** are more stable than **4**, the barriers for the attack of the second ligand are greater for them. Since the energies of the transition states and intermediates are not so large in comparison to those for **4**, other isomers may also be formed in the reaction mixture.

The attack of the second ligand at the other shared boron atoms **G** and **H** have barriers of 25.9 (**11AG**) and 26.5 kcal/mol (**11AH**), respectively. The structures, where both of the ligands are at shared boron atoms, **4AG** and **4AH** are found to be minima (Figure 5). They do not have the *closo/nido* pattern but have two quadrilateral open faces. We have not studied these any further.

The reaction initiated by the attack of the ligand at the BIII atom of $B_{20}H_{16}$ (**7**, Figure 3) leads to the intermediate **10B**, which is 15.7 kcal/mol higher in energy than the reactants. The attack of the second ligand at the **BIV** of **10B** through a transition state **11BA** with a barrier of 20.4 kcal/mol leads to the intermediate **12AB.** This shows that for the
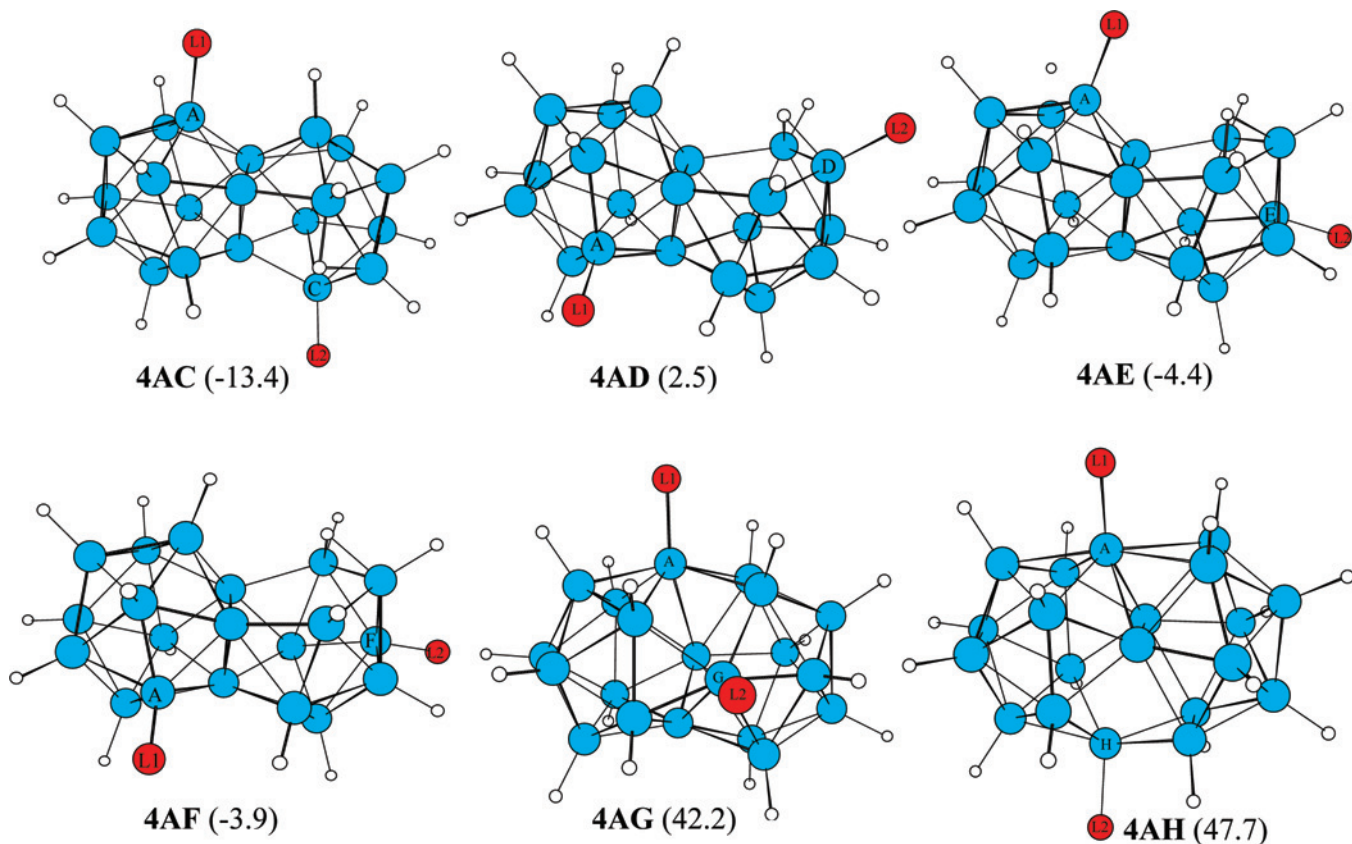
Figure 5. Optimized geometries of other possible isomers of $B_{20}H_{16}L_2$. Energies relative to **4** are given in parenthases.
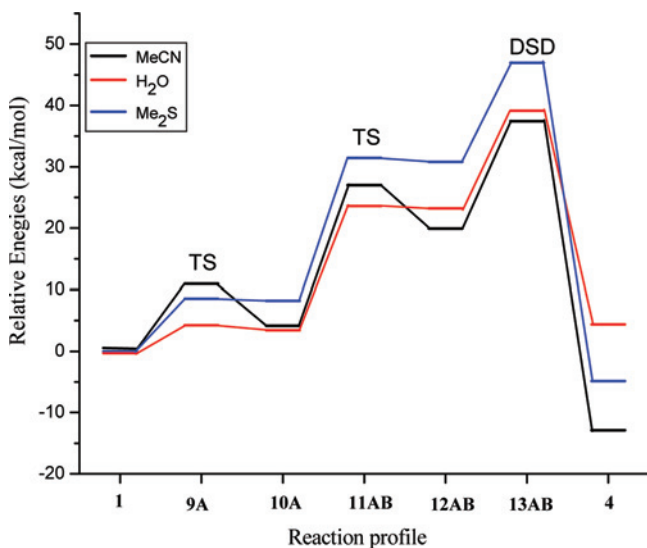

Figure 6. Reaction profile for the cage opening of $B_{20}H_{16}$ in the presence of ligands, L = MeCN, H_2O, and Me_2S.

Table 2. Relative Energies (kcal/mol) Calculated at the B3LYP/6-31G* Level When L = MeCN, H_2O, and Me_2S

structure	L = MeCN	L = H_2O	L = Me_2S
1	0.0	0.0	0.0
9A (TS)	10.9	4.2	8.6
10A	4.7	3.4	8.2
11AB (TS)	27.1	23.6	31.4
12AB	19.9	23.2	30.8
13AB (DSD)	37.4	39.2	46.9
4	−12.9	4.4	−4.9

10A are found to be 20.3 and 23.2 kcal/mol, respectively. The barriers for the DSD rearrangements (Figure 6) are calculated to be 16.0 and 16.2 kcal/mol for the H_2O and the Me_2S, respectively. The product **4** is lower in energy than the reactants for L = Me_2S and slightly higher in energy for L = H_2O. The *closo/nido* structure $B_{20}H_{16}(H_2O)_2$ (**14**, Figure 7) undergoes further hydrolysis resulting in $[B_{20}H_{16}(OH)_2]^{2-}$-$2[H_3O]^{+}$.[3c] The optimization of $[B_{20}H_{16}(OH)_2]^{2-}$ retains the *closo/nido* structure (**15**, Figure 7).

The computational study shows that the cage-opening reactions of $B_{20}H_{16}$ are multistep processes. The first intermediate **10A** requires a low barrier (10.9 kcal/mol) of formation, and the transition state for the addition of the second ligand is much higher in energy (22.9 kcal/mol). In view of this, the first intermediate **10A** may be observable in an experiment, where concentration of the MeCN and temperature are controlled.

Conclusions

The reaction of $B_{20}H_{16}$ with ligands L = MeCN, H_2O, and Me_2S is studied theoretically. We propose a mechanism

formation of the intermediate **12AB** through **9A**, **10AB** and **11AB** are energetically more feasible.

The most feasible reaction path (**9A → 10A → 11AB → 12AB → 13AB → 4**) for the reaction of $B_{20}H_{16}$ is also studied for the other ligands L = H_2O and Me_2S (Figure 6). The reaction is initiated by nucleophilic attack through the O and S atoms of the ligands H_2O and Me_2S, respectively. The barriers for the formation of **10A** are calculated to be 4.2 (H_2O) and 8.6 kcal/mol (Me_2S), respectively (Table 2). The barriers for the second attack of the ligand at the **B** atom of

14
B$_{20}$H$_{16}$(H$_2$O)

15
[B$_{20}$H$_{16}$(OH)$_2$]$^{2-}$

Figure 7. Deprotonation of *closo/nido* B$_{20}$H$_{16}$(H$_2$O)$_2$ into *closo/nido* [B$_{20}$H$_{16}$(OH)$_2$]$^{2-}$.

for the ring opening of B$_{20}$H$_{16}$ to a face shared *closo/nido* macropolyhedron through a diamond-square-diamond rearrangement. The formation of the product by the addition of two MeCN molecules to B$_{20}$H$_{16}$ is thermodynamically more stable than that by the addition of H$_2$O or Me$_2$S. Even though only one isomer of the product has been reported experimentally, calculations predict the possibility of the formation of other isomers as well.

Supporting Information Available: Listing of total energies and Cartesian coordinates of all structures. This material is available free of charge via the Internet at http://pubs.acs.org.

IC702509J